Available online at www.sciencedirect.com
ScienceDirect
C. R. Mecanique 337 (2009) 141–149
COMPTES RENDUS MECANIQUE

On the heat and mass transfer analogy for natural convection of non-dilute binary mixtures of ideal gases in cavities

Hua Sun, Guy Lauriat *

Université Paris-Est, laboratoire de modélisation et simulation multi-échelle (MSME FRE-CNRS 3160), 5, boulevard Descartes, Champs sur Marne, 77454 Marne-la-Vallée cedex 2, France

Received 14 November 2008; accepted after revision 1 April 2009

Presented by Sébastien Candel

Abstract

An extension of a slightly compressible flow model to double-diffusive convection of a binary mixture of ideal gases enclosed in a cavity is presented. The problem formulation is based on a low Mach number approximation and the impermeable surface assumption is not invoked. The main objectives of this paper are the statement of a new problem formulation, and the analysis of some significant results showing the influence of density variations on transient solutions for pure thermal or pure solutal convection. At steady-state, it is shown that the heat and mass transfer analogy may be applied for non-dilute mixtures at parameter ranges larger than those usually considered. ***To cite this article: H. Sun, G. Lauriat, C. R. Mecanique 337 (2009).***
© 2009 Académie des sciences. Published by Elsevier Masson SAS. All rights reserved.

Résumé

Sur l'analogie transfert de chaleur et de matière pour la convection naturelle de mélanges binaires non-dilués de gaz parfaits. Le modèle d'écoulement faiblement compressible est étendu à la convection doublement diffusive d'un mélange binaire de gaz parfaits contenus dans une cavité. L'écriture des équations de conservation et de la loi d'état du mélange s'appuie sur une approximation "bas Mach" en tenant compte des vitesses de diffusion sur les parois. Les objectifs de cet article sont de proposer une nouvelle formulation du problème et de discuter quelques résultats significatifs. Les cas de convection thermique et de convection solutale sont considérés successivement. On montre que l'analogie transfert de chaleur–transfert de matière reste applicable dans des domaines de paramètres plus étendus que ceux habituellement admis. ***Pour citer cet article : H. Sun, G. Lauriat, C. R. Mecanique 337 (2009).***
© 2009 Académie des sciences. Published by Elsevier Masson SAS. All rights reserved.

Keywords: Computational fluid mechanics; Thermosolutal convection; Low-Mach number flows

Mots-clés : Mécanique des fluides numériques ; Convection thermosolutale ; Ecoulements faiblement compressibles

* Corresponding author.
E-mail addresses: hua.sun@univ-paris-est.fr (H. Sun), lauriat@univ-paris-est.fr (G. Lauriat).

1631-0721/$ – see front matter © 2009 Académie des sciences. Published by Elsevier Masson SAS. All rights reserved.
doi:10.1016/j.crme.2009.04.001

1. Introduction

Double-diffusive (or thermosolutal) convection occurs when buoyancy forces are due both to temperature and concentration gradients. Many flow structures are possible depending on how temperature and concentration gradients are oriented relative to gravity. Double diffusive natural convection in enclosures filled with dilute binary mixtures has been investigated extensively both experimentally and numerically. The main objectives of many of the works published in the heat and mass transfer literature were the analysis of the flow structure, and the Nusselt and Sherwood numbers as functions of dimensionless parameters. Thermal natural convection in gas filled cavities in which large density gradients exist was solved by employing weakly compressible flow models by Leonardi and Reizes [1], and Zhong et al. [2], amongst others. The more recent numerical study by Vierendeels et al. [3] as well as the solutions compared within the framework of a benchmark problem (Le Quéré et al. [4,5]) were based on the low-Mach number formulation, first introduced by Paolucci [6].

In the present study, this formulation is applied to non-isothermal, non-dilute binary mixture cavity flows subjected to large variations in density for ideal gas mixtures. The impermeable surface assumption is not invoked in order to account for the mass flux advected at the vertical walls. The heat and mass transfer analogy and the influences of the initial thermodynamic conditions on steady-state solutions are discussed.

2. Problem formulation

The geometry investigated is illustrated in Fig. 1. Natural convection is driven by thermal and/or solutal horizontal gradients. The flow is assumed to be laminar, there are no chemical reactions, heat generation or heat dissipation, and radiative heat transfer across the enclosure is neglected. The heat flux driven by mass fraction gradients (Dufour effect) and the mass flux driven by temperature gradients (Soret effect) as well as species interdiffusion are neglected. Since the present study is focused on the effects of density variations, the changes in the other thermophysical properties of the mixture with temperature and mass fraction are not accounted for in order to reduce the number of parameters. At initial state, the cavity is assumed to be filled with a mixture at uniform temperature and concentration fields.

Various boundary conditions may be applied for the energy and species conservation equations, as stated in the current literature (see for example Weaver and Viskanta [7] and Bird et al. [8]). For the momentum equation, the impermeable surface model is restricted to dilute binary mixture for which mass transfer–heat transfer analogy is relevant. This assumption is by definition an approximation because mass diffusion always produces convection.

2.1. Thermal convection in a rectangular 2D-cavity

Thermal convection in a vertical, differentially heated cavity is investigated first. Fig. 1(a) shows a schematic diagram of the cavity and applied boundary conditions. Uniform hot and cold temperatures, T_h and T_c are specified at the vertical walls and the horizontal boundaries are adiabatic. The scales for length, velocity and temperature difference are chosen as the cavity width, L, the thermal diffusion velocity $u_d = a_r/L$ (where $a_r = k_r/\rho_r C_{p,r}$ is the reference thermal diffusivity) and the maximum temperature difference $\Delta T = T_h - T_c$, respectively. The governing equations are thus cast in dimensionless form by using the following dimensionless variables

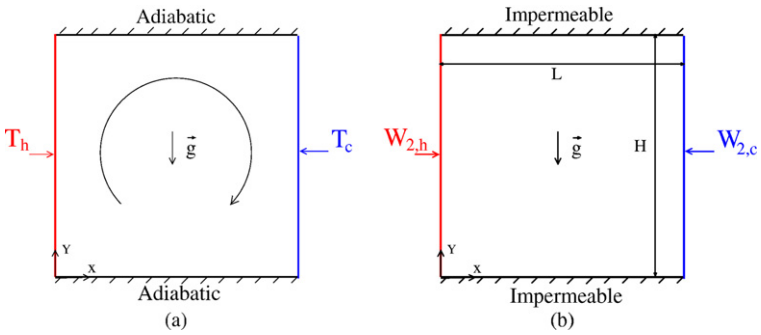

Fig. 1. Schematic diagram of the rectangular cavity. (a) thermal natural convection, (b) solutal natural convection.

$$x^* = \frac{x}{L}, \quad y^* = \frac{y}{L}, \quad \tau = \frac{tu_d}{L}, \quad \rho^* = \frac{\rho_m}{\rho_r}, \quad p^* = \frac{p'_m}{\rho_r u_d^2}, \quad \overline{P}^* = \frac{\overline{P}}{\overline{P}_r}$$
$$u^* = \frac{u}{u_d}, \quad v^* = \frac{v}{u_d}, \quad \theta = \frac{T - T_r}{\Delta T} \tag{1}$$

where T_r is assumed to be the average of the vertical wall temperatures for $t > 0$. p'_m is the motion pressure and $\overline{P}$ the thermodynamic pressure. Based on the constant thermophysical property assumption except density, the resulting dimensionless conservation equations are:

$$\frac{\partial \rho^*}{\partial \tau} + \nabla \cdot (\rho^* \vec{V}^*) = 0 \tag{2}$$
$$\frac{\partial (\rho^* \vec{V}^*)}{\partial \tau} + \nabla \cdot (\rho^* \vec{V}^* \otimes \vec{V}^*) = -\nabla p^* + Pr \nabla \cdot \bar{\bar{\tau}}^* + \frac{1}{Fr_T}(\rho^* - 1)\frac{\vec{g}}{|\vec{g}|} \tag{3}$$
$$\frac{\partial (\rho^* \theta)}{\partial \tau} + \nabla \cdot (\rho^* \vec{V}^* \theta) = \nabla^2 \theta + \frac{(\gamma - 1)}{\gamma \epsilon_T} \frac{\mathrm{d}\overline{P^*}}{\mathrm{d}\tau} \tag{4}$$

where $Fr_T = a_r^2 / g L^3$ is the thermally based Froude number, $Pr = \mu_r C_{p,r} / k_r$ is the Prandtl number, $\gamma = C_p / C_v$ is the ratio of specific heats. $\epsilon_T = \Delta T / T_r$ characterizes the thermal deviation from the Boussinesq approximation. For a cavity filled with an ideal gas, the dimensionless thermodynamic pressure may be written as

$$\overline{P}^*(\tau) = \frac{A}{\int_0^A \int_0^1 (\frac{1}{\epsilon_T \theta + 1}) \, \mathrm{d}x^* \, \mathrm{d}y^*} \tag{5}$$

In the above expression, $A = H/L$ is the cavity aspect ratio. The local dimensionless fluid density is obtained from the perfect gas law as follows

$$\rho^* = \frac{\overline{P}^*(\tau)}{1 + \epsilon_T \theta} \tag{6}$$

The dimensionless initial and boundary conditions are

$$u^* = v^* = 0, \quad \theta = \theta_0 \quad \text{at } \tau = 0, \ \forall x^*, y^* \tag{7}$$
$$u^* = v^* = 0, \quad \theta = \pm 0.5 \quad \text{at } x^* = 0, 1 \text{ for } \tau > 0, \ \forall y^* \tag{8}$$
$$u^* = v^* = 0, \quad \partial\theta / \partial y^* = 0 \quad \text{at } y^* = 0, A \text{ for } \tau > 0, \ \forall x^* \tag{9}$$

The local Nusselt number at the hot wall is defined as

$$Nu(y^*) = -\left.\frac{\partial \theta}{\partial x^*}\right|_{x^*=0} \tag{10}$$

At steady-state, the average Nusselt numbers at the hot and cold walls must be equal whatever the initial conditions.

2.1.1. Effects of initial conditions on the steady-state solution.

Since the overall mass of fluid is constant, the reference density should be evaluated at a well-defined reference state. The average density is generally not known at T_r. Therefore, care should be taken when assuming constant thermal properties except density if the initial temperature is not the average of wall temperatures (i.e. $T_r \neq T_0$ or $\theta_0 \neq 0$). Although the Prandtl number may be assumed constant over a large temperature range for ideal gases, the Froude number must be calculated by using data for the thermal conductivity and specific heat at the average wall temperature (i.e. T_r), while the reference density is that at the initial thermodynamic conditions (i.e. for T_0 and $\overline{P}_0$). It follows that

$$\rho_r = \rho_0, \quad \overline{P}_r = \overline{P}_0 \quad \text{and} \quad \overline{P}^*(\tau) = \frac{A}{\int_0^A \int_0^1 (\frac{\epsilon_T \theta_0 + 1}{\epsilon_T \theta + 1}) \, \mathrm{d}x^* \, \mathrm{d}y^*} \quad \text{if } \theta_0 \neq 0 \tag{11}$$

For the present non-Boussinesq formulation based on a constant thermophysical property assumption, except density, the solution depends thus on six dimensionless parameters (A, Fr_T, Pr, γ, ϵ_T, θ_0).

2.2. Solutal convection in a rectangular 2D-cavity

Solutal convection in a vertical cavity with different uniform mass fractions of species "2" suddenly imposed at the vertical walls is investigated in what follows. An inert carrier gas (species "1") which does not diffuse into the walls is present in the cavity. Fig. 1(b) shows a schematic diagram of the cavity and applied boundary conditions. Uniform mass fractions, $W_{2,h}$ and $W_{2,c}$, are specified at the vertical left-hand side and right-hand side walls. It is assumed here that $W_{2,h} > W_{2,c}$. Zero species fluxes are prescribed at the horizontal boundaries. Depending on the molecular weight ratio, $M^* = M_2/M_1$, the solutal body force produces either a clockwise fluid circulation ($M^* < 1$) or a trigonometric circulation ($M^* > 1$). The scale for mass fraction difference is the maximum mass fraction difference, $\Delta W_2 = W_{2,h} - W_{2,c}$. The velocity scale is based on the solutal diffusion velocity $u_d = D_{12}/L$. The governing equations are thus cast in dimensionless form by using the following set of dimensionless variables

$$x^* = \frac{x}{L}, \quad y^* = \frac{y}{L}, \quad \tau = \frac{t u_d}{L}, \quad \rho^* = \frac{\rho_m}{\rho_0}, \quad p^* = \frac{p'_m}{\rho_0 u_d^2}, \quad \overline{P}^* = \frac{\overline{P}}{\overline{P}_0}$$
$$u^* = \frac{u}{u_d}, \quad v^* = \frac{v}{u_d}, \quad W_2^* = \frac{W_2 - W_{2,r}}{\Delta W_2} \tag{12}$$

where $W_{2,r}$ is the average of the vertical walls values for $t > 0$. It should be emphasized that the overall mass of fluid present into the cavity cannot be known whatever $t > 0$, owing to the different mass flux rates at the walls in transient régime (except for extremely dilute binary mixtures for which the mass may be assumed constant and equal to the one of the carrier gas). Therefore, the reference density cannot generally be defined at the reference conditions used for the other physical properties. We retained thus the density at initial state. Based on the constant thermophysical property assumption except mixture density, the resulting dimensionless conservation equations are:

$$\frac{\partial \rho^*}{\partial \tau} + \nabla \cdot (\rho^* \vec{V}^*) = 0 \tag{13}$$
$$\frac{\partial (\rho^* \vec{V}^*)}{\partial \tau} + \nabla \cdot (\rho^* \vec{V}^* \otimes \vec{V}^*) = -\nabla p^* + Sc \nabla \cdot \bar{\bar{\tau}}^* + \frac{1}{Fr_S}(\rho^* - 1)\frac{\vec{g}}{|\vec{g}|} \tag{14}$$
$$\frac{\partial (\rho^* W_2^*)}{\partial \tau} + \nabla \cdot (\rho^* \vec{V}^* W_2^*) = \nabla \cdot (\rho^* \nabla W_2^*) \tag{15}$$

where $Fr_S = D_{12}^2/gL^3$ is the solutal Froude number and $Sc = \mu_r/\rho_0 D_{12}$ is the Schmidt number. The mass diffusion coefficient depends on the thermodynamic pressure (see the Chapman–Enskog formula [8], for example). On the other hand, the results of the kinetic gas theory show that the Schmidt number may be assumed constant since μ is proportional to $\sqrt{T}$. Consequently, the two dimensionless parameters involved in the steady-state conservation equations for thermal (Fr_T and Pr) and solutal (Fr_S and Sc) convection behave similarly. The dimensionless thermodynamic pressure based on mass conservation may be written as

$$\overline{P}^*(\tau) = \frac{1}{\int_0^A \int_0^1 (\frac{\epsilon_m W_{2,0}^* + 1}{\epsilon_m W_2^* + 1})\, \mathrm{d}x^* \, \mathrm{d}y^*} \left\{ A + \Delta M_2(\tau) \right\} \tag{16}$$

In the above expression, subscript "0" refers to the initial conditions and ϵ_m characterizes the solutal deviation from the usual assumption of binary dilute solutions. It reads

$$\epsilon_m = \frac{(1 - M^*)\Delta W_2}{M^* + (1 - M^*) W_{2,r}} \tag{17}$$

The term $\Delta M_2(\tau)$ denotes the mass of species "2" added within the cavity between times $\tau = 0$ and τ due to mass diffusion at the walls. It is zero if both species diffuse into the walls while it is given by

$$\Delta M_2(\tau) = -\frac{1}{C_w - 0.5} \int_0^\tau \int_0^A \rho^* \frac{\partial W_2^*}{\partial x^*}\bigg|_{x^*=0} \mathrm{d}y^* \, \mathrm{d}\tau + \frac{1}{C_w + 0.5} \int_0^\tau \int_0^A \rho^* \frac{\partial W_2^*}{\partial x^*}\bigg|_{x^*=1} \mathrm{d}y^* \, \mathrm{d}\tau \tag{18}$$

provided that the mass of species "1" present in the enclosure is constant. It is worth noting that $\Delta M_2(\tau)$ vanishes at steady state. In the right-hand side of Eq. (18), $C_w = (1 - W_{2,r})/\Delta W_2$. The local dimensionless mixture density is obtained from the ideal gas law as follows

$$\rho^* = \frac{\overline{P}^*(\tau)}{1 + \epsilon_m W_2^*} \tag{19}$$

The dimensionless initial and boundary conditions are

$$u^* = v^* = 0, \quad W_2^* = W_{2,0}^* \quad \text{at } \tau = 0, \ \forall x^*, y^* \tag{20}$$

$$u^* = -\frac{1}{C_w \mp 0.5} \frac{\partial W_2^*}{\partial x^*}\bigg|_{0,1}, \quad v^* = 0, \quad W_2^* = \pm 0.5 \quad \text{at } x^* = 0, 1 \text{ for } \tau > 0, \ \forall y^* \tag{21}$$

$$u^* = v^* = 0, \quad \frac{\partial W_2^*}{\partial y^*} = 0 \quad \text{at } y^* = 0, A \text{ for } \tau > 0, \ \forall x^* \tag{22}$$

It should be underlined that the introduction of non-zero initial conditions ($W_{2,0}^* \neq 0$) automatically implies a dependence of the steady-state solution with the initial state as it can be deduced from Eqs. (16) and (20). The mass fluxes at the vertical walls are the sum of a diffusion term and an advection term due to the normal velocities produced by the mass fluxes at the surfaces. Hence, the local Sherwood number at the LHS-wall is defined as

$$Sh(y^*) = -\rho^* \frac{\partial W_2^*}{\partial x^*}\bigg|_{x^*=0} + \rho^* u^* W_2^*(0, y^*) = Sh_{\text{diff}} + Sh_{\text{adv}} \tag{23}$$

At steady-state, the average Sherwood numbers at the vertical walls must be equal owing to the boundary conditions applied at the horizontal surfaces. It should be noted that the average Sherwood number can be related to the total dimensionless mass flux through a vertical wall $\dot{m}^* = \int_0^A \rho^* u^* \, \mathrm{d}y^*$ as

$$\overline{Sh} = C_w \dot{m}^* \tag{24}$$

while the advective part of the average Sherwood number is related to the mass flux as follows

$$\overline{Sh}_{\text{adv}} = \frac{1}{2} \dot{m}^* \tag{25}$$

For the present non-Boussinesq solutal formulation based on a constant thermophysical property assumption, except mixture density, the solutions depend on six dimensionless parameters (A, Fr_S, Sc, ϵ_m, C_w, $W_{2,0}^*$).

2.3. Thermosolutal convection in a rectangular 2D-cavity

The non-Boussinesq formulation for thermosolutal convection can be readily derived by combining the above systems of conservation equations. The dimensionless thermodynamic pressure and density may be obtained from the following relationships:

$$\overline{P}^*(\tau) = \frac{1}{\int_0^A \int_0^1 (\frac{\epsilon_T \theta_0 + 1}{\epsilon_T \theta + 1})(\frac{\epsilon_m W_{2,0}^* + 1}{\epsilon_m W_2^* + 1}) \, \mathrm{d}x^* \, \mathrm{d}y^*} \big\{ A + \Delta M_2(\tau) \big\} \tag{26}$$

$$\rho^* = \frac{\overline{P}^*(\tau)}{(1 + \epsilon_T \theta)(1 + \epsilon_m W_2^*)} \tag{27}$$

The relationship for the local Sherwood number (Eq. (23)) is not modified. On the other hand, an advective term must be added into the local Nusselt number such as:

$$Nu(y^*, \tau) = -\frac{\partial \theta}{\partial x^*}\bigg|_{x^*=0} + 0.5 \rho^* u^* = Nu_{\text{diff}} + Nu_{\text{adv}} \tag{28}$$

The non-Boussinesq thermosolutal formulation based on a constant thermophysical property assumption, except mixture density, involves thus ten dimensionless parameters: A, C_w, Fr, Le, Pr, γ, ϵ_T, ϵ_m, θ_0 and $W_{2,0}^*$. Such a number of parameters together with the possibility of combined or opposed buoyancy effects is therefore a severe limitation for a complete analysis of thermosolutal natural convection in cavities.

As can be seen from Eqs. (5) and (16), the dimensionless steady-state thermodynamic pressure tends towards unity if $\epsilon_T \to 0$ or if $\epsilon_m \to 0$. Therefore, the Boussinesq approximation is recovered for $\epsilon_T \ll 1$ and $\epsilon_m \ll 1$ and it can be readily shown that this approximation leads to constant thermodynamic pressure and density (except in the buoyancy term). For subcritical laminar flows, the dimensionless steady-state velocity, temperature and mass fraction fields are thus independent on the initial conditions.

For large values of ϵ_m and ϵ_T, the constant property assumption is highly questionable. However, the changes to bring to the above problem formulation is straightforward: all the dimensionless parameters must be evaluated at the same thermodynamic state, and appropriate dimensionless functions must be introduced in the diffusion terms. For the specific case of wet walls with liquid water, relevant formulas can be found in Tsilingiris [12], for example.

2.4. Numerical resolution

The finite volume method was employed to discretize the system of conservation equations on staggered, non-uniform Cartesian grids with a second-order central difference scheme for the convective terms. The IDEAL algorithm recently proposed by Sun et al. [9] for incompressible fluid flow and heat transfer was used to solve the velocity–pressure coupling. In the present work the IDEAL algorithm was extended to weakly compressible, thermosolutal flows without under-relaxation factors for u^*, v^* and p^*. The time integration was conducted with an Alternating Direction Implicit scheme (ADI), and at each time step there existed an inner doubly iterative process for obtaining the pressure field solution. The time step was chosen such that the maximum value of the Courant–Friedrichs–Lewis number (CFL) was of the order of one. A mesh study was conducted by using non-uniform grids having from 64×64 to 512×512 nodes. For the range of parameters considered in the present work, a 256×256 grid represents a good compromise between accuracy and computational costs. The adopted convergence criterion required that relative maximum mass and field variable residuals were less than 10^{-9}. A coarse estimate of the leading order of the truncation error can also readily be calculated as $N_x^{-1.97}$, showing an overall second-order spatial accuracy of the scheme. Comparisons of the results obtained for large temperature difference ($\epsilon_T = 1.2$) and $Ra_T = 10^6$ was made with those by Vierendeels et al. [3] and with the recent benchmark solutions reported in Le Quéré et al. [4,5]. The most accurate results were recovered within three digits for the average quantities reported in [3,5].

3. Results and discussion

For a specified geometry, the full analogy exists only if the energy and mass species conservation equations and boundary conditions are similar in dimensionless form. Since the pressure term in the energy equation is zero at steady-state, it is relevant to determine the conditions for which $\overline{Nu} = \overline{Sh}$ for non-dilute flow solutions in a cavity with uniform but different temperatures or mass fractions at the walls.

To this end, we investigated the time evolutions of $\overline{Nu}$ and $\overline{Sh}$ for various values of ϵ_T and ϵ_m in the case of pure thermal and pure solutal flows by starting from the same zero initial conditions for a fluid at rest ($\theta_0 = W^*_{2,0} = 0$, i.e. $T_0 = T_r$ and $W_{2,0} = W_{2,r}$). When using the low Mach number formulation, the Froude number was varied as $Fr_T = 10^{-6}\epsilon_T/Pr$ for the thermal cases ($Pr = 0.71$) and as $Fr_S = 10^{-6}\epsilon_m/Sc$ for the solutal cases with $Sc = Pr$. When the Boussinesq approximation is invoked, $Ra_T = Ra_m = 10^6$ and the average Nusselt numbers at the vertical walls are equal in the transient regime owing to the zero initial conditions.

In the thermal boundary layer regime, it is well established that the Boussinesq steady-state flows are not reached by a monotonous transition if the computations are started from a fluid at rest. The flow displays an oscillatory behaviour which corresponds to a typical time-periodic motion, as it has been investigated in detail by Patterson and Imberger [10] who presented a scale analysis which agrees very well with many published numerical works. For a square differentially heated vertical cavity, the dimensionless period of the oscillatory behaviour is close to $\tilde{p} = 2\pi\sqrt{2/Ra_T Pr}$.

Figs. 2 and 3 display the effect of the non-Boussinesq parameters on the evolutions of the mean Nusselt and Sherwood numbers for purely thermal or solutal convection. In the range of ϵ_T-variation considered, Fig. 2 and Table 1 show that the steady-state $\overline{Nu}$ does not differ much from the Boussinesq value ($\overline{Nu} = 8.83$). As it has been shown in Laaroussi and Lauriat [11], this result is directly linked to the choice of the initial thermodynamic conditions used for these computations ($\theta_0 = 0$, $\overline{P}^*(0) = 1$). On the other hand, although the frequency of the oscillatory behaviour is not significantly modified when varying ϵ_T, the mean Nusselt numbers at the cold and hot walls exhibit large

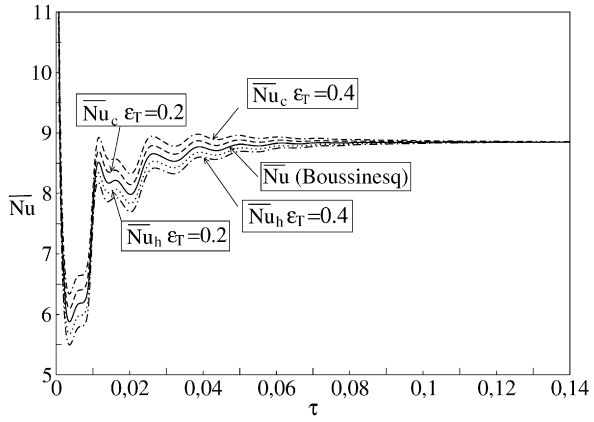

Fig. 2. Transient variations of the average Nusselt numbers at the cold and hot walls as a function of ϵ_T ($Ra_T = 10^6$, $Pr = 0.71$, $A = 1$, $\gamma = 1.4$, $\theta_0 = 0$).

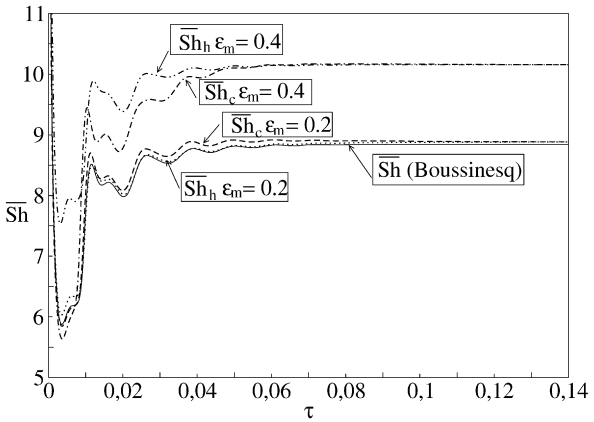

Fig. 3. Transient variations of the average Sherwood numbers at the walls as a function of ϵ_m for pure solutal convection ($Ra_m = 10^6$, $Sc = 0.71$, $A = 1$, $M^* = 0.6$, $W^*_{2,0} = 0$, $C_w = 2.5$ for $\epsilon_m = 0.2$ and $C_w = 0.83$ for $\epsilon_m = 0.4$).

Table 1
Steady-state average Nusselt number and thermodynamic pressure for various values of the non-Boussinesq parameter ϵ_T ($A = 1$, $Pr = 0.71$, $Fr_T = 10^{-6}\epsilon_T/Pr$ or $Ra_T = 10^6$, $\gamma = 1.4$, $\theta_0 = 0$).

	Boussinesq	$\epsilon_T = 0.1$	$\epsilon_T = 0.2$	$\epsilon_T = 0.3$	$\epsilon_T = 0.4$
$\overline{Nu}$	8.826	8.827	8.828	8.829	8.831
$\overline{P}^*$	1.0	0.999	0.996	0.992	0.986

differences, $\overline{Nu}_c$ being larger than $\overline{Nu}_h$. Plots of any primitive variable at any point within the cavity show that the period ($\tilde{p} = 0.011$) agrees well with the theoretical predictions.

Fig. 3 shows the evolutions of the mean Sherwood numbers at the walls for various values of ϵ_m in the specific case $M^* = 0.6$ (humid air) and $W_{2,c} = 0$ (dry right-hand side wall). As expected, $\overline{Sh} = \overline{Nu}$ for binary dilute solution (Boussinesq approximation and $Le = 1$). Therefore the heat and mass transfer analogy is fulfilled at any time. For $\epsilon_m \geqslant\approx 0.1$, the first main difference between thermal and solutal flows lies in the increases in both the wall Sherwood numbers which are greater than for the dilute case. Second, $\overline{Sh}_c$ may be either smaller or larger than $\overline{Sh}_h$ according to the ϵ_m and C_w-values. As can be seen, the steady-state values differ all the more since ϵ_m increases. The explanation is that the advective mass fluxes at the walls increase with ϵ_m since $C_w = [(1 - M^*) - 0.5\epsilon_m]/\epsilon_m M^*$, if $W_{2,c} = 0$. About the oscillatory behaviour, Fig. 3 shows that the frequencies are surprisingly almost the same although the velocity boundary conditions are not identical when considering pure thermal or pure solutal cases.

Table 2
Steady-state Sherwood number, thermodynamic pressure, average density and mass flow rates $\dot{m}^*$ through the vertical walls for various values of the solutal non-Boussinesq parameter ϵ_m at constant C_w ($A = 1$, $Sc = 0.71$, $Fr_S = 10^{-6}\epsilon_m/Sc$ or $Ra_m = 10^6$, $W^*_{2,0} = 0$, $C_w = 5.83$).

	Boussinesq	$\epsilon_m = 0.1$	$\epsilon_m = 0.2$	$\epsilon_m = 0.3$	$\epsilon_m = 0.4$
$\overline{Sh}$	8.826	8.826	8.771	8.703	8.619
$\overline{P}^*$	1.0	0.999	0.992	0.981	0.967
$\overline{\rho}^*$	1.0	0.999	0.996	0.993	0.990
$\dot{m}^*$	0	1.513	1.505	1.493	1.479

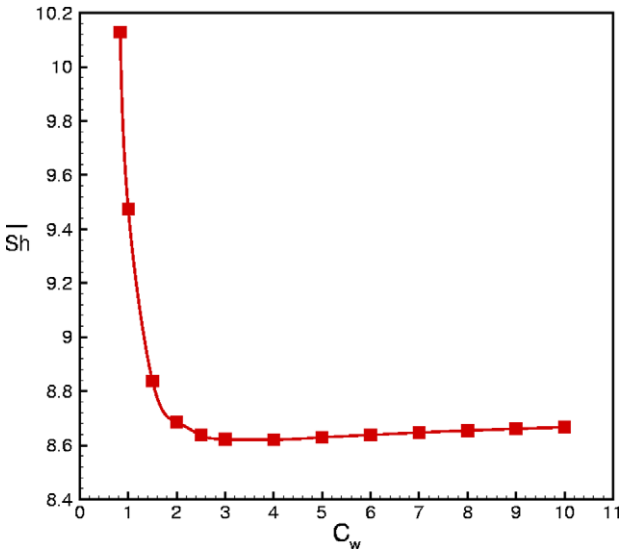

Fig. 4. Variation of the mean Sherwood number with the wall-parameter ($A = 1$, $Ra_m = 10^6$, $Sc = 0.71$, $M^* = 0.6$, $W^*_{2,0} = 0$ and $\epsilon_m = 0.4$).

Table 3
Steady-state Sherwood number, thermodynamic pressure, average density and mass flow rates $\dot{m}^*$ through the vertical walls for various values of the solutal non-Boussinesq parameter ϵ_m at constant M ($A = 1$, $M^* = 0.6$, $Sc = 0.71$, $Fr_S = 10^{-6}\epsilon_m/Sc$ or $Ra_m = 10^6$, $W^*_{2,0} = 0$, $\Delta W_2 = 2W_{2,r}$, $C_w = 5.83$, 2.5, 1.39, and 0.83).

	Boussinesq	$\epsilon_m = 0.1$	$\epsilon_m = 0.2$	$\epsilon_m = 0.3$	$\epsilon_m = 0.4$
$\overline{Sh}$	8.826	8.826	8.864	9.086	10.129
$\overline{P}^*$	1.0	0.999	0.997	1.002	1.051
$\overline{\rho}^*$	1.0	0.999	0.998	1.002	1.038
$\dot{m}^*$	0	1.513	3.546	6.542	12.154

The results reported in Table 2 show that the Sherwood number decreases slightly as the solutal parameter increases, unlike to what is predicted for thermal convection. It should be noted that the computations were carried out for a quite large C_w value in order to consider small effects of the mass flux rates at the walls. The advective part of the Sherwood number (Eq. (25)) is therefore small in comparison with its diffusive part. The small variations with the non-Boussinesq parameters both in $\overline{Nu}$ and $\overline{Sh}$ leads to conclude that the heat and mass transfer analogy still holds within the range of changes in ϵ_m and ϵ_T considered.

For a fixed set of the other solutal parameters, blowing and suction effects at the walls increase as the wall parameter C_w decreases towards its asymptotic value ($C_w = 0.5$). Its magnitude is obviously linked to the mass fraction difference between the walls, so that changes in C_w while keeping ϵ_m constant imply changes in the mixture components. Fig. 4 shows that the blowing and suction effects may be assumed negligible for $C_w > 2$ while they produce a sharp increases in $\overline{Sh}$ for smaller C_w-values. By combining the variations in ϵ_m and C_w (i.e for a given binary mixture or M^*), large increases in the mass transfer may be predicted, as exemplified in Table 3.

4. Conclusion

Variable density effects on natural convection in a vertical cavity filled with a binary mixture of ideal gases are numerically investigated by using a weakly compressible flow model. The study is conducted in the case where an inert carrier gas (species "1") present in the cavity is not soluble in species "2", and do not diffuse into the walls (evaporation of water vapor in dry air for example).

Under these conditions, mixture density and thermodynamic pressure experience significant changes from initial to steady states. However, in the range of parameters investigated, it is shown that the average steady Nusselt and Sherwood numbers do not differ significantly provided that the mass flux advected at the wall is much smaller than the mass diffusion flux. Therefore, the heat and mass transfer analogy can be considered as valid for solutal and thermal parameters (ϵ_m and ϵ_T, respectively) few times larger than the 0.1-limit usually reported in the current literature. A new problem formulation is proposed for solving thermosolutal convection with large density variations.

References

[1] E. Leonardi, J.A. Reizes, Natural convection in compressible fluids with variable properties, in: R.W. Lewis, K. Morgan (Eds.), Numerical Methods in Thermal Problems, vol. 1, Pineridge Press, 1979, pp. 297–306.
[2] Z.Y. Zhong, K.T. Yang, J.R. Lloyd, Variable properties effects in laminar natural convection in a square enclosure, ASME J. Heat Transfer 107 (1985) 133–138.
[3] J. Vierendeels, B. Merci, E. Dick, Numerical study of natural convective heat transfer with large temperature differences, Int. J. Numer. Methods Heat Fluid Flows 11 (4) (2001) 329–341.
[4] P. Le Quéré, C. Weisman, H. Pallière, J. Vierendeels, E. Dick, R. Becker, M. Braack, J. Locke, Modelling of natural convection flows with large temperature differences: A benchmark problem for low Mach number solvers, Part 1. References solutions, ESAIM Math. Model. Numer. Anal. 39 (3) (2005) 609–616.
[5] P. Le Quéré, C. Weisman, H. Pallière, J. Vierendeels, E. Dick, R. Becker, M. Braack, J. Locke, Modelling of natural convection flows with large temperature differences: A benchmark problem for low Mach number solvers, Part 2. Contributions to the June 2004 Conference, ESAIM Math. Model. Numer. Anal. 39 (3) (2005) 617–621.
[6] S. Paolucci, On the filtering of sound from the Navier–Stokes equations, Technical report, Sandia National Laboratory, 1982, SAND82-8257.
[7] J.A. Weaver, R. Viskanta, Natural convection due to horizontal temperature and concentration gradients: 1. Variable thermophysical properties effects, Int. J. Heat Mass Transfer 34 (12) (1991) 3107–3120.
[8] R.B. Bird, W.E. Stewart, E.N. Lightfoot, Transport Phenomena, second ed., Wiley and Sons, 2007.
[9] D.L. Sun, Z.G. Qu, Y.L. He, W.Q. Tao, An efficient segregated algorithm for incompressible fluid flow and heat transfer problems – IDEAL (Inner Doubly iterative Efficient Algorithm for Linked equations). Part 1: Mathematical formulation and solution procedure, Numer. Heat Transfer, Part B 53 (2008) 1–17.
[10] J. Patterson, J. Imberger, Unsteady natural convection in a rectangular cavity, J. Fluid Mech. 100 (1980) 65–86.
[11] N. Laaroussi, G. Lauriat, Conjugate thermosolutal convection and condensation of humid air in cavities, Int. J. Thermal Sci. 47 (2008) 1571–1586.
[12] P.T. Tsilingiris, Thermophysical and transport properties of humid air at temperature range between 0 and 100 °C, Energy Conversion and Management 49 (2008) 1098–1110.